Available online at www.sciencedirect.com
SCIENCE DIRECT®
Precambrian Research 126 (2003) 331–348
Precambrian Research
www.elsevier.com/locate/precamres

Graphite and carbonates in the 3.8 Ga old Isua Supracrustal Belt, southern West Greenland

Mark A. van Zuilen [a,*], Aivo Lepland [b], Jane Teranes [a], John Finarelli [c], Martin Wahlen [a], Gustaf Arrhenius [a]

[a] *Scripps Institution of Oceanography, University of California San Diego, La Jolla, San Diego, CA 92093-0236, USA*
[b] *Geological Survey of Norway, Leiv Eirikssons vei 39, Trondheim 7491, Norway*
[c] *Committee on Evolutionary Biology, University of Chicago, 1025 E. 57th Street Culver Hall 402, Chicago, IL 60637, USA*

Accepted 5 February 2003

Abstract

We present a systematic study of abundance, isotopic composition and petrographic associations of graphite in rocks from the ca. 3.8 Ga Isua Supracrustal Belt (ISB) in southern West Greenland. Most of the graphite in the ISB occurs in carbonate-rich metasomatic rocks (metacarbonates) while sedimentary units, including banded iron formations (BIFs) and metacherts, have exceedingly low graphite concentrations. Regardless of isotopic composition of graphite in metacarbonate rocks, their secondary origin disqualifies them from providing evidence for traces of life stemming from 3.8 Ga. Recognition of the secondary origin of Isua metacarbonates thus calls for reevaluation of earlier interpretations that suggested the occurrence of 3.8 Ga biogenic graphite in these rocks. Thermal decomposition of siderite; $6FeCO_3 = 2Fe_3O_4 + 5CO_2 + C$, is the process seemingly responsible for the graphite formation. The cation composition (Fe, Mg, Mn, and Ca) of the carbonate minerals, carbon isotope ratios of carbonates and associated graphite and petrographic assemblages of a suite of metacarbonates support the conclusion that multiple pulses of metasomatism affected the ISB, causing the deposition of Fe-bearing carbonates and subsequent partial disproportionation to graphite and magnetite. Equilibrium isotope fractionation between carbonate and graphite in the rocks indicates peak metamorphic temperatures between 500 and 600 °C, in agreement with other estimates of metamorphic temperature for the ISB. Published by Elsevier B.V.

Keywords: Archean; Isua; Graphite; Carbon isotope ratio; Biomarker; Metacarbonate

1. Introduction

The search for evidence of the earliest life on Earth is hindered by the poor preservation of the Early Archean rock record. The very few exposed supracrustal formations that date back beyond 3.5 Ga, have all been subjected to high or intermediate grade metamorphism, which would distort morphological microfossils beyond recognition, and alter organic matter to kerogen and, ultimately, to crystalline graphite.

The search for life in >3.5 Ga rocks therefore relies entirely on chemical and isotopic indicators. The ratio of carbon isotopes ($^{13}C/^{12}C$) is commonly used to infer a biogenic origin for reduced carbon in sediments. Unfortunately, the original depleted isotopic signature of organic matter can be altered by metamorphic processes (Hayes et al., 1983). For instance, isotope exchange between organic matter and carbonates, as

* Corresponding author. Present address: Centre de Recherches Pétrographiques et Géochimiques B.P. 20, 54501 Vandoeuvre les Nancy Cedex, France.
E-mail address: markvz@crpg.cnrs-nancy.fr (M.A. van Zuilen).

0301-9268/$ – see front matter. Published by Elsevier B.V.
doi:10.1016/S0301-9268(03)00103-7

well as volatilization processes during organic matter maturation, will lead to a shift towards higher $\delta^{13}C$ values and loss of a characteristic biogenic isotope signature.

Researchers have long alleged that graphite contained in amphibolite grade rocks from the 3.8 Ga Isua Supracrustal Belt (ISB) in southern West Greenland could be biogenic in origin (Schidlowski et al., 1979; Schidlowski, 1988, 2001; Mojzsis et al., 1996). The wide range of carbon isotope ratios ($\delta^{13}C$ range from −25 to −6‰) of graphite in carbonate-rich rocks has been interpreted to reflect post-depositional isotopic equilibration of graphitizing organic matter with coexisting carbonates. This equilibration scenario was also applied as an explanation for the carbon isotopic composition of Isua carbonates, whose $\delta^{13}C$ values are somewhat lower than typical $\delta^{13}C$ values from unmetamorphosed carbonate deposits found throughout the geological record. Schidlowski (1988) concluded that "there is little doubt that the Isua values have been reset by metamorphism, and that the isotopic signature of autotrophic carbon fixation originally extended back at least to Isua times."

Protoliths of several Isua rock types have been reinterpreted since the original study of Schidlowski et al. (1979). Carbonate-rich Isua lithologies were proven to have a secondary, metasomatic origin (Rose et al., 1996; Rosing et al., 1996), and not sedimentary as had been thought previously. This fundamental reinterpretation of the protolith would rule out a biogenic origin of graphite in carbonate-rich rocks and exclude the possibility that graphite serves as a primary 3.8 Ga biomarker in these rocks. Several studies (Nagy et al., 1975; Perry and Ahmad, 1977; Dymek and Klein, 1988; Naraoka et al., 1996) have highlighted the possibility of an abiogenic origin of the graphite encountered in the ISB, and have proposed various epigenetic mechanisms of formation. Here we describe the typical field appearance of some metacarbonate outcrops and present the petrography and isotopic composition of graphite in a suite of representative samples. We also present data on the coexisting carbonate phases, including cation compositions and carbon isotope ratios. Our data, the related discussion of isotopic systematics, and the recent evidence for extensive metasomatism allow an in-depth reinterpretation of the mechanism for graphite formation in Isua metacarbonates. Ultimately, these new findings draw into question the potential of graphite as a biomarker for ancient life in Isua rocks. Some of the related data have been presented in our earlier publications (Lepland et al., 2002; van Zuilen et al., 2002).

2. Geology of the Isua Supracrustal Belt

The ISB is part of the 3.8 Ga Itsaq Gneiss Complex in southern West Greenland, and represents one of the earliest records of a hydrosphere on Earth (Moorbath et al., 1973; Nutman et al., 1996). Initial field mapping of the ISB led to the recognition of a stratigraphy, folded into an upright isoclinal syncline. The stratigraphy was divided into nine formations consisting of metavolcanic and metasedimentary rocks, intruded by ultramafic and mafic bodies (Nutman, 1986; Nutman et al., 1984). Sedimentary units recognized in the ISB, included conglomerates, banded iron formations (BIFs), metacherts, and felsic metasediments in which graded bedding is locally preserved. The occurrences of siderite and dolomite (metacarbonates), occasionally interlayered with quartzite in the ISB appeared similar to marine platform deposits that are found throughout the Precambrian and the Phanerozoic, and led to the interpretation of a shallow marine, subtidal depositional environment in Isua (Dimroth, 1982; Nutman et al., 1984).

Recent mapping efforts (Appel et al., 1998; Komiya et al., 1999; Fedo, 2000; Myers and Crowley, 2000; Fedo et al., 2001; Myers, 2001) have shown that the initial interpretation of stratigraphy and protoliths in the ISB needed revision. Pillow lava structures were recognized in many outcrops that were previously interpreted as mafic intrusions (Appel et al., 1998; Komiya et al., 1999). Metacarbonates and calc-silicate rocks in the ISB were typically found in close association with ultramafic rocks, often forming envelopes around the igneous bodies (Rosing et al., 1996).

Several carbonate occurrences were found to have a replacive nature; e.g. carbonate contacts cross-cutting pre-existing lamination, evidence of fluid advection along fractures, carbonate interfingering with host rock lithologies. Rose et al. (1996) proposed a geochemical model in which a metamorphic fluid flows through an ultramafic body (dunite) that is embedded between two layers of host rock. Initially the composition of the fluid is determined by the local equilibrium

with the mineral phases of the host rock. As the fluid flows into the ultramafic body it will deposit SiO_2, Al_2O_3 and CO_2, causing a local alteration of the ultramafic body to a talc–magnesite–chlorite schist. This alteration considerably reduces the SiO_2 activity of the fluid. The fluid re-equilibration with the host rock at the downstream contact leads to formation of a mineral assemblage characteristic for calc-silicate Isua rocks. The geochemical modeling thus agrees with the field evidence showing development of carbonated zones downstream of the contact where the fluid exits the ultramafic body. As was noted by Rosing and Rose (1993) and Rose et al. (1996), metacarbonates are not invariably found in contact with ultramafic rocks. Fluids may migrate for some distance along faults and fractures before reacting with country rock to form metacarbonate zones. The presence of carbonate zones on strike with an ultramafic body could indirectly point to a genetic relationship.

It is now widely accepted that much of the lithological diversity in the ISB can be explained as a result of the metasomatic fluid–rock reactions of a small number of protolith compositions under amphibolite-facies metamorphic conditions. Carbonate-rich Isua lithologies including rocks that were previously considered to represent carbonate facies BIF are probably all metasomatic in origin. Undisputed metasedimentary units such as BIFs, metacherts, conglomerates and graded beds, have a limited patchy distribution in the ISB. The largest outcrops of metasediments occur in the north-eastern part of the ISB (Fig. 1), within a zone of relatively low strain (Appel et al., 1998; Fedo, 2000). The unambiguous recognition of primary depositional features in this zone makes this a preferable area to search for ancient remnants of life. Metasedimentary rocks of turbiditic and pelagic origin with Bouma sequence depositional features (Rosing, 1999) have been recognized in a zone of relatively low strain in the western part of the belt.

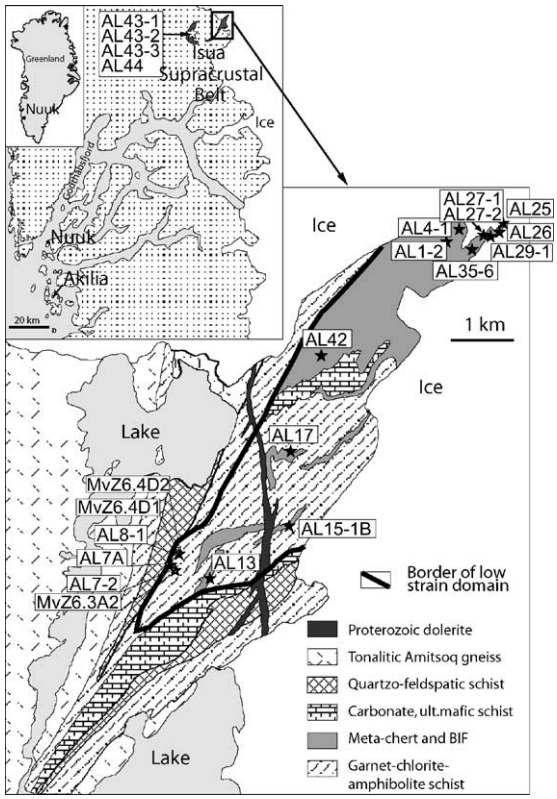

Fig. 1. Simplified geologic map (after Appel et al., 1998) of the eastern part of the Isua Supracrustal Belt in southern West Greenland. Most of the samples were collected from the 'low-strain zone' in the northeastern part of the ISB including metacarbonates (AL17, AL7-2, AL8-1, AL7A, MvZ6.3A2, MvZ6.4D1, MvZ6.4D2), BIFs (AL4-1, AL27-1, AL27-2, AL13, AL35-6, AL15-1B), metacherts (AL25, AL26, AL42) and mafic dykes (AL1-2, AL29-1). Three samples from a metasedimentary turbidite sequence (AL43-1, AL43-2, AL43-3) as well as a metacarbonate sample (AL44) from the western part of the belt were also studied. Metacarbonate sample AL7-2 was subdivided into a magnetite-rich band (AL7-2M) and a carbonate-rich band (AL7-2C). Sample AL17 represents heavily metasomatized chert. Subsamples from both carbonate dominated (AL17C) and chert dominated (AL17Chert) bands were analyzed.

3. Materials

A set of samples including metacarbonates, BIFs, metacherts and mafic dykes from the 'low-strain zone' in the northeastern part of the ISB (Fig. 1; Table 1) were obtained during two field seasons. Three samples from a metasedimentary turbidite sequence (two from slates (AL43-1, AL43-3) and one (AL43-2) from a graded bed between these units) as well as a metacarbonate sample (AL44) from the western part of the belt (Fig. 1) were also included. Most of the discussion in this paper concerns metacarbonates; data on other rock types are given for comparison. We apply the term "metacarbonate" to concordant or cross-cutting carbonate-rich veins. Many metasedimentary rocks,

Table 1
Sample description, results CHN-analysis and carbon isotope analysis

Sample	Latitude	Longitude	Rock type	$C_{graphite}$ (wt.%)	$\delta^{13}C_{carbonate}$	$\delta^{13}C_{graphite}$	$\Delta^{13}C_{carbonate-graphite}$
AL13	65°09.94′	49°48.88′	BIF	<d.l.	1.12		
AL15-1B	65°10.12′	49°48.52′	BIF	<d.l.	–[a]		
AL27-1	65°12.64′	49°45.37′	BIF	<d.l.	−6.54		
AL27-2	65°12.64′	49°45.37′	BIF	<d.l.	−6.65		
AL35-6	65°12.53′	49°45.60′	BIF	<d.l.	−8.97		
AL4-1	65°12.58′	49°45.73′	BIF	<d.l.	–[a]		
AL25	65°12.73′	49°45.09′	Chert	<d.l.	−4.44		
AL26	65°12.68′	49°45.15′	Chert	<d.l.	–[a]		
AL42	65°11.35′	49°47.77′	Chert	<d.l.	−4.91		
AL1-2	65°12.46′	49°46.04′	Mafic dyke	<d.l.	−4.81		
AL29-1	65°12.63′	49°45.26′	Mafic dyke	<d.l.	−5.97		
AL43-1	65°08.83′	50°10.11′	Turbidite	0.26	−8.70	−18.17	9.47
AL43-2	65°08.83′	50°10.11′	Turbidite	0.13	−7.30	−19.04	11.74
AL43-3	65°08.83′	50°10.11′	Turbidite	0.20	−9.79	−18.64	8.85
AL44	65°07.67′	50°10.95′	Metacarbonate	0.94	−4.36	−10.14	5.79
AL7-2C	65°10.01′	49.50.25′	Metacarbonate	0.71	−1.13	−10.80	9.66
AL7-2M	65°10.01′	49°50.25′	Metacarbonate	0.23	−2.52	−11.43	8.91
AL7A	65°10.01′	49°50.33′	Metacarbonate	0.30	−6.54	−12.46	5.92
AL8-1	65°10.12′	49°50.26′	Metacarbonate	1.00	−7.57	−11.84	4.27
AL17C	65°10.76′	49°48.51′	Metacarbonate	0.50	−3.29	−9.26	5.97
AL17Chert	65°10.76′	49°48.51′	Metacarbonate	0.39	–[b]	−8.81	5.52
MvZ6.3A2	65°10.01′	49°50.12′	Metacarbonate	2.06	−1.44	−10.49	9.06
MvZ6.4D1	65°10.12′	49°50.26′	Metacarbonate	1.90	–[a]	−11.44	
MvZ6.4D2	65°10.12′	49°50.26′	Metacarbonate	1.68	–[a]	−11.06	

<d.l.: below detection limit of CHN-analysis.
[a] Samples contain no carbonate.
[b] As sample AL17C.

e.g. BIFs and metacherts, also contain small amounts (<5%) of carbonate minerals as small veinlets, but the original texture and composition of these rocks have not been significantly altered by metasomatism. Samples MvZ6.4D1 and MvZ6.4D2 are highly graphitic, chlorite and magnetite-dominated interlayers within MgMn-siderite-rich metacarbonate veins. These samples are therefore also treated as metacarbonates in this study. Metacarbonate samples were derived from centimeter- to meter-scale conspicuous brown, rust colored (due to weathering/oxidation of Fe-carbonate) veins, typically occurring within metavolcanic garnet–chlorite amphibolite schists (Fig. 2). Although quartz banding is lacking, locally abundant streaks of magnetite in these carbonate veins occasionally causes them to resemble heavily weathered bands of BIF (Fig. 6a). Siderite is commonly found in many Archean and Proterozoic BIFs, and rocks with pure quartz–siderite banding are considered a separate facies of BIF (James, 1954). It is likely that many carbonate-rich metasomatic veins in the ISB were originally mapped as BIFs that formed part of the sedimentary sequence. In fact Appel (1980) recognized a type of ‘carbonate facies BIF’ (c.f. James, 1954) in the ISB, which was described to consist of layers of magnesium- and manganese-rich siderite, with occasional thin magnetite-rich bands. Appel noted that quartz is characteristically absent in these rocks, and that graphite is interstitial to siderite, but may be found enclosed in magnetite and siderite as well. Dymek and Klein (1988), who made a detailed study of iron-rich rocks in Isua, also recognized carbonate-rich iron formations that had high concentrations of graphite. Based on its field appearance they distinguished a specific type of iron formation as “... slaty or fissile rocks containing abundant but variable magnetite and graphite. Such ‘graphitic iron formation’ forms meter-thick lenticular, highly weathered (commonly to chocolate brown) outcrops of uncertain lateral extent.” It was further noted that these graphitic iron formations

Fig. 2. Typical examples of graphitic, magnetite-rich metacarbonate veins in amphibolite–chlorite–garnet schist country rock, interpreted as metamorphosed ocean floor basalts. (a) Location for samples AL7-2 and MvZ6.3A2. (b) Close-up of the pinched-out vein shown in (a). (c) Location for sample AL7A.

contained high amounts of MgO, which suggested to Dymek and Klein (1988) that Mg–Fe-carbonates may have been important early constituents.

4. Methods

4.1. Carbonate

Analysis of the cation composition (Fe, Mg, Mn, and Ca) of the carbonate minerals was performed by energy dispersive spectrometry (EDS) on a Cambridge S-360 scanning electron microscope (SEM) using thin sections. Ratios of each cation to total cations in carbonate were obtained from the X-ray spectra, and were used for calculation of empirical formulae for the carbonate species of each sample.

The well-established CO_2 liberation method (concentrated anhydrous H_3PO_4 at 25 °C; McCrea, 1950) for isotopic determination of calcite is not suitable for iron-rich dolomites and siderites, due to their low reaction rates at low temperature (Rosenbaum and

Sheppard, 1986). Isua rocks contain several types of carbonate minerals with different resistance to acid. This presents further challenges to accurate isotopic determination, as partial reaction can result in isotopic fractionation and/or bias the analysis toward fast reacting minor carbonate constituents.

We determined the carbon isotope ratio of carbonates on ground powders (<30 μm grain size) by reacting them with concentrated H_3PO_4 at 90 °C and collecting the evolved CO_2 on a liquid nitrogen cold finger. By monitoring evolved CO_2 with a pressure gauge over the reaction chamber, we insured that the reaction was carried to completion, i.e. until no measurable amount of CO_2 was being evolved (a minimum of 1.5 h). To ensure complete decomposition of the most acid-resistant carbonate phases the reaction time was extended for 1 h beyond apparent completion, while collecting any residual CO_2 on the cold finger. However, in no case were such traces of remnant reacting carbonate detected. The evolved and frozen CO_2, was cryogenically cleaned to remove SO_2 and H_2O, and then transferred to an Isogas precision isotope ratio mass spectrometer (PRISM) for isotopic determination. Error bars of measurements are 0.1‰.

4.2. Graphite

Rock powders (<30 μm grain size) were decarbonated in 4 M HCl at 70 °C for 48 h. The amount of graphite in the acid treated rock powders was determined by CHN-analysis (ultra-precision balance and Perkin-Elmer 2400 CHN Elemental Analyzer; 0.1 wt.% detection limit) and subsequent corrections were made for the weight loss incurred at acid treatment.

Prior to carbon isotope analysis, soluble organic contaminants were removed by washing the decarbonated powders three times in a 10:1 mixture of dichloromethane:ethanol. Samples were wrapped in pure (99.99%) Pt-foil and put in 9 mm Vycor tubes, together with 100 mg CuO. Before use, the Vycor tubes were heated in a muffle furnace at 900 °C for 4 h. Samples were pre-oxidized at 300 °C for 15 min, and then sealed under vacuum. The samples were combusted at 900 °C for 5 h. Evolved CO_2 gas was frozen on a cold finger with liquid nitrogen. Using a variable heater immersed in liquid nitrogen, CO_2 was liberated at −135 °C, while keeping SO_2 and H_2O frozen. The liberated CO_2 was further purified by passing the gas through two Pyrex coils immersed in an ethanol–liquid nitrogen mixture at −94 °C. The purified CO_2 was isolated in a Pyrex tube and transferred to a VG PRISM-II multicollector mass spectrometer for isotope analysis. All measurements were corrected for ^{17}O (Craig, 1957), and for blank contributions. The blank correction calculation was made according to Wedeking et al. (1983). An operational blank (combustion with Pt-foil and CuO at 900 °C for 5 h and subsequent processing in the vacuum extraction line) typically produced 1 μl CO_2, with a $\delta^{13}C = -27 \pm 0.05$‰. Sample sizes were chosen such that more than 100 μl CO_2 was produced (typical sample size 500 μl). Due to this precaution the blank correction was always smaller than 0.15‰. Error bars are smaller than 0.2‰, based on twice the standard deviation of four standard preparations and measurements (graphite standard, USGS24).

5. Results

5.1. Cation composition and carbon isotope ratio of carbonates

Using SEM-EDS analysis, we divided the carbonate phases in the Isua rocks into three distinct groups based on their carbonate cation compositions (Fig. 3): (1) iron-deficient carbonate (calcite; $Fe_{0.02–0.08}Mg_{0.00–0.03}Mn_{0.01–0.04}Ca_{0.89–0.97}CO_3$), found in veinlets within BIF, metachert and turbidite sequence samples (Fig. 3a), (2) carbonates with moderate iron content (Fe-dolomite; $Fe_{0.09–0.36}Mg_{0.14–0.34}Mn_{0.00–0.06}Ca_{0.50–0.57}CO_3$), found in metacarbonates AL8-1 (population b) and (AL17C), and in small veinlets within some BIFs and metacherts (Fig. 3b) and (3) iron-rich carbonate (MgMn-siderite; $Fe_{0.40–0.85}Mg_{0.03–0.40}Mn_{0.09–0.22}CO_3$), found only in metacarbonate samples from veins occurring as distinct layers in mafic metavolcanic country rock (Fig. 3c).

The occurrence of MgMn-siderite in veins within mafic rocks likely reflects the interaction between carbonate-rich metasomatic fluids and Fe-rich country rocks. Some samples contained two distinct carbonate compositions: Fe-dolomite and calcite in AL17C, AL27-1, AL42 and MgMn-siderite and Fe-dolomite in AL8-1. The occurrence of different compositions

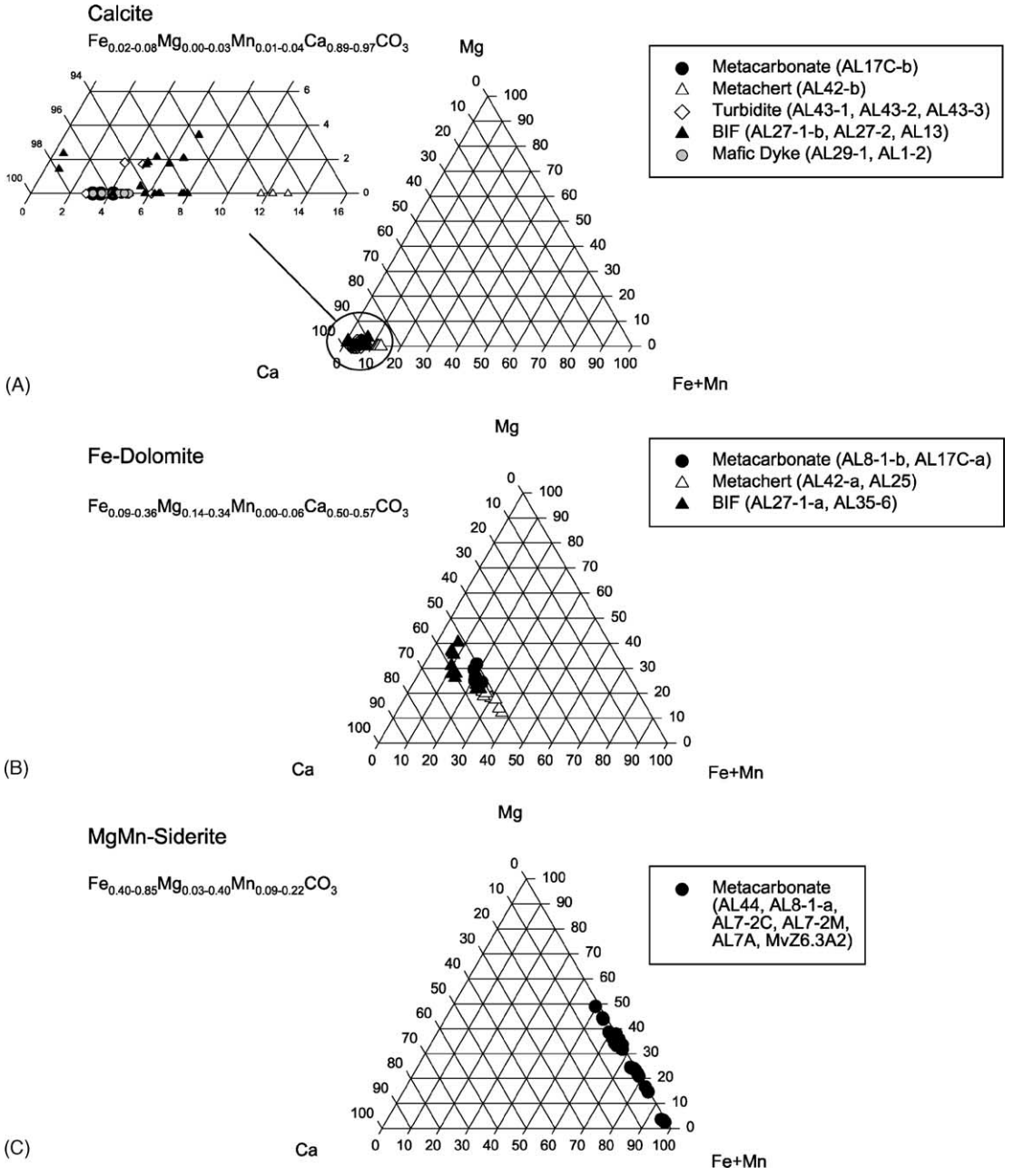

Fig. 3. SEM-EDS determined carbonate cation composition. Three carbonate spot analyses per sample. Triangular plots Fe + Mn–Mg–Ca show that carbonate phases fall into three different compositional types: Calcite, Fe-dolomite, and MgMn-siderite. Some samples (AL8-1, AL17C, AL27-1, AL42) contain carbonate with two different compositions, indicated by populations "a" and "b". The samples AL15-1B, AL4-1, AL26, MvZ6.4D1, MvZ6.4D2 are not shown on this figure because they do not contain carbonate or no carbonate minerals could be identified in thin sections. In our previous publication (van Zuilen et al., 2002) sample AL13 was erroneously reported not to contain carbonate. Here we report the cation composition of carbonate from this sample. This result does not affect any of the conclusions in the previous paper.

on a centimetre-scale (observed within thin sections) suggests that different pulses of metasomatism, each pulse depositing a carbonate of a specific composition, influenced these rocks. The isotopic composition of the carbonate carbon ranges between +1 and −9‰ (Fig. 4; Table 1). These values represent total carbonate in the sample. There seems to be no relation between $\delta^{13}C$ value and carbonate composition. On average, these values (average $\delta^{13}C = -5.2‰$) are slightly lighter than the average value ($\delta^{13}C = -2.5‰$) previously reported by Schidlowski et al. (1979).

5.2. Abundance and isotopic composition of graphite

CHN analyses revealed measurable amounts (>0.1 wt.%) of graphite only in metacarbonate and turbidite samples, where graphite concentrations varied between 0.3 and 2 wt.%, and between 0.15 and 0.3 wt.%, respectively (Fig. 5a; Table 1). In contrast, graphite concentrations in BIFs and metacherts were below the detection limit of CHN analysis. Low graphite abundances in BIFs and metacherts (<5 ppm) have been confirmed by high precision stepped-combustion measurements (van Zuilen et al., 2002). The isotopic composition of bulk graphite in the metacarbonate samples ranges from −12 to −9‰ (Fig. 5b; Table 1). The $\delta^{13}C$ values of graphite are significantly lower in turbidite samples, varying between −18 and −19‰. Determination of bulk graphite isotopic composition in BIFs and metacherts was impractical due to the virtual absence of graphite in these samples. Stepped-combustion experiments on these samples demonstrated that of the small amount of reduced carbon present, practically all is contained in recent, unmetamorphosed organic matter (van Zuilen et al., 2002).

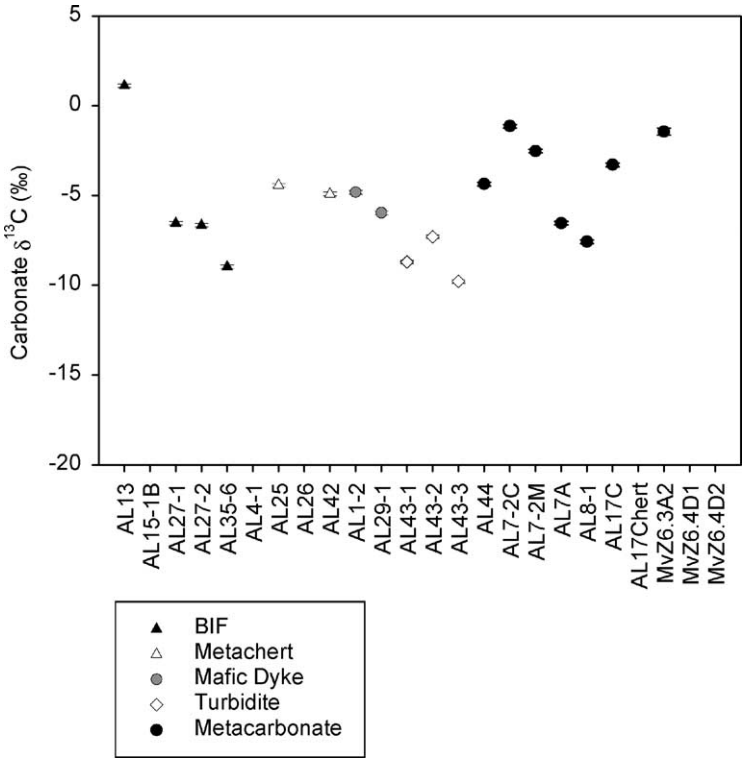

Fig. 4. Carbon isotopic composition of carbonate phases. Values represent total carbonate. No data are shown for AL15-1B, AL4-1, AL26, MvZ6.4D1 and MvZ6.4D2 because these samples do not contain carbonate; the chert dominated part of metacarbonate sample AL17 (AL17Chert) was not analysed for carbon isotopes on carbonate.

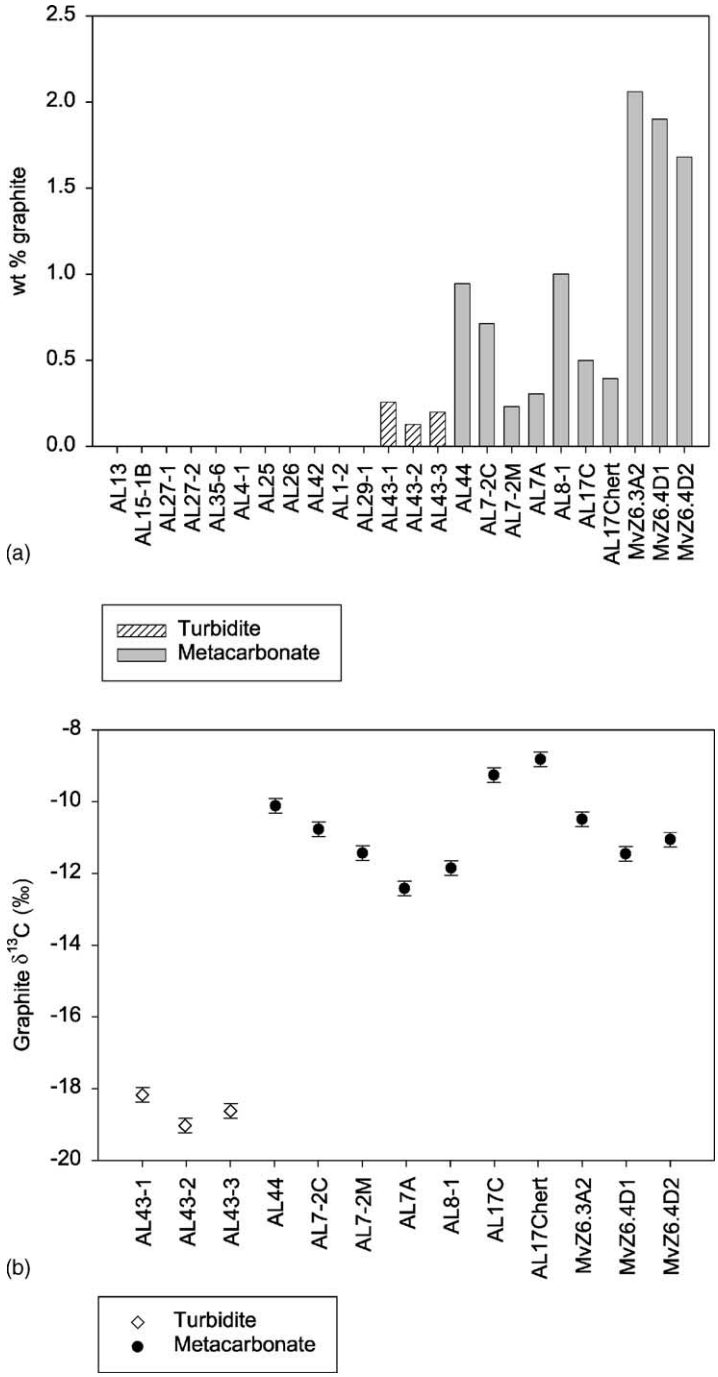

Fig. 5. (a) Graphite abundance (wt.%). (b) Carbon isotopic composition of graphite. Graphite abundance in metasedimentary BIFs and metacherts (AL13 to AL42) and mafic dykes (AL1-2 and AL29-1) are beyond detection limit of CHN technique (<0.1%).

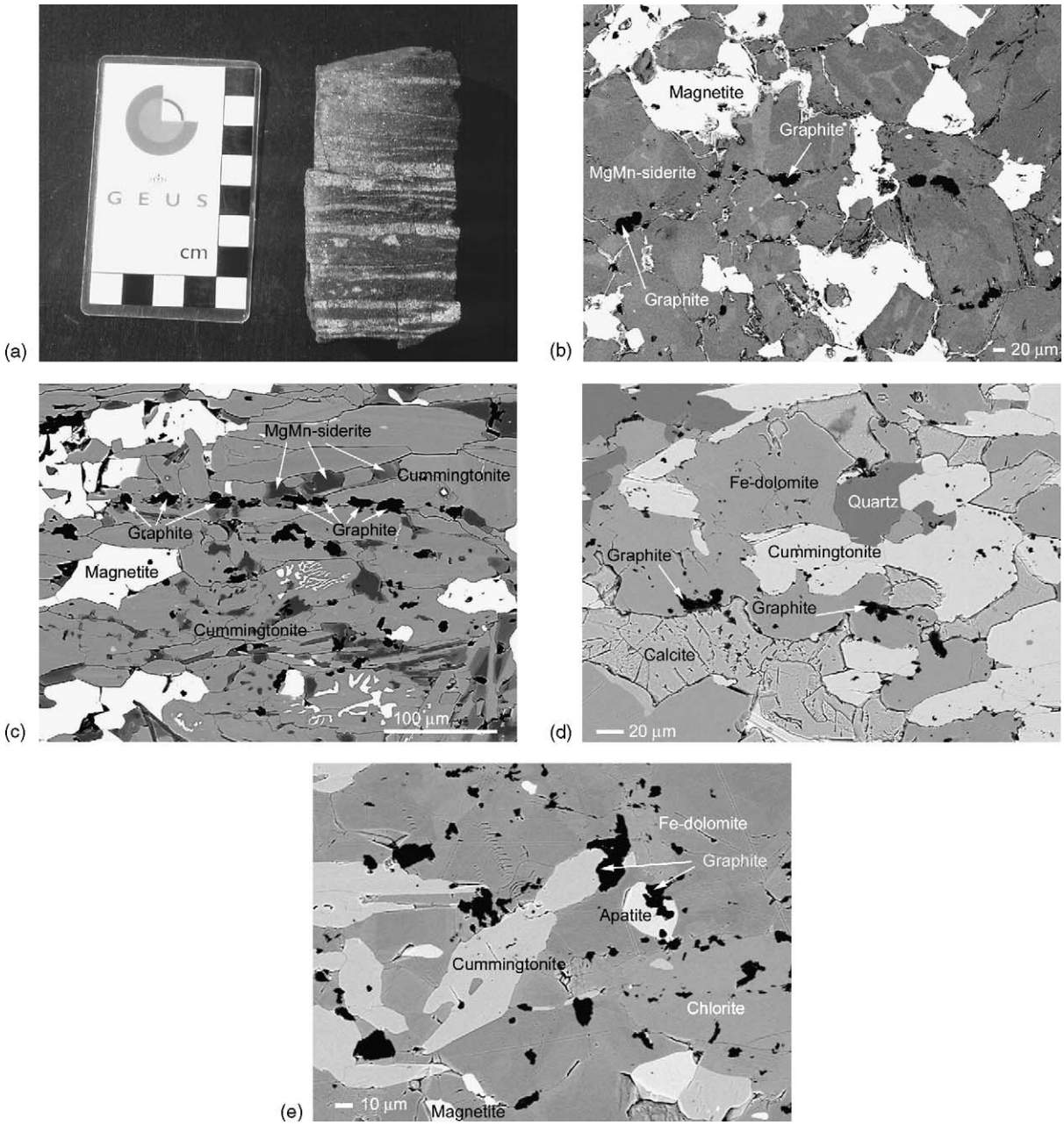

Fig. 6. (a) Hand specimen of metacarbonate AL44 showing alteration of grey bands rich in magnetite and garnet and brown bands rich in MgMn-siderite, magnetite and graphite. (b) SEM-BSE-image showing the petrographic association of MgMn-siderite–magnetite–graphite in one of the brown bands shown in (a). (c) SEM-BSE-image of sample AL8-1 showing an MgMn-siderite–magnetite–graphite association. (d) SEM-BSE-image of a carbonate-rich band of sample AL17 showing graphite in relation to calcite, Fe-dolomite and cummingtonite. (e) SEM-BSE-image of sample AL8-1 showing graphite in apatite as well as in other surrounding mineral phases.

5.3. Petrographic analysis

Micropetrographic analysis revealed that graphite in metacarbonates typically occurs in close association with Fe-bearing carbonate (MgMn-carbonate or Fe-dolomite) and magnetite (Fig. 6a–c). This mineral association was seen in all metacarbonate veins in mafic country rocks. In a metacarbonate vein within metachert (AL17C and AL17Chert) graphite was found in association with Fe-dolomite and cummingtonite (Fig. 6d). Two samples from a chlorite-dominated interlayer in a metacarbonate vein (MvZ6.4D1 and MvZ6.4D2) contain abundant graphite and magnetite, but no carbonate.

6. Discussion

6.1. Origin of graphite in metacarbonate veins

The occurrence of graphite in metacarbonate veins in close association with Fe-bearing carbonate and magnetite suggests a genetic relationship between these phases. Such a mineral assemblage can be produced metamorphically from the thermal disproportionation of siderite to magnetite ($FeO{\cdot}Fe_2O_3$; Fe_3O_4) resulting in reduction of the carbonate ion. Siderite breaks down according to the reaction:

$$3FeCO_3 = Fe_3O_4 + 2CO_2 + CO \quad (1)$$

The produced CO_2:CO ratio 2:1 is metastable with respect to graphite at temperatures between 400 and 600 °C (Muan, 1958). Therefore, as siderite decomposes, graphite precipitates from the gas phase according to the reaction:

$$2CO = C + CO_2 \quad (2)$$

The overall reaction can be expressed as:

$$6FeCO_3 = 2Fe_3O_4 + C + 5CO_2 \quad (3)$$

In the Fe–C–O system this four-phase assemblage (siderite–magnetite–graphite–gas) defines a unique equilibrium temperature at a fixed gas pressure. For instance, at a pressure of 500 bar this equilibrium assemblage defines a temperature of 455 °C, at an oxygen fugacity $fO_2 = 10^{-25.7}$ bar (French, 1971). Siderite decomposition experiments have been carried out for a wide range of P and T conditions (French and Eugster, 1965; French and Rosenberg, 1965; Yui, 1966; French, 1971; Weidner, 1972; Mel'nik, 1982). Most of these experiments were carried out in closed tubes, in which the oxygen buffer was established directly by the precipitation of graphite. The univariant curves of the siderite–magnetite–graphite–gas equilibria from these different experiments are plotted in a P–T diagram (Fig. 7). The open-tube experiments of French and Rosenberg (1965) are considered most precise, because the fO_2 was fixed by an external buffer. The data by Weidner (1972), based on closed-tube experiments using $CO + CO_2$ gas (which should fix fO_2 by the graphite–gas buffer), show equilibrium temperatures that are ca. 100 °C higher than the data by French and Rosenberg (1965). The difference between these two datasets is discussed in detail in French (1971) and Weidner (1972), but a definite explanation is not given. The results of French and Rosenberg (1965) are here taken as the minimum and those of Weidner (1972) as the maximum temperatures at which siderite decomposes under metamorphic conditions. Under natural conditions many factors influence the P–T conditions of this equilibrium. Substitution of Mg, Mn, and Ca for Fe will stabilize iron-rich carbonates at higher temperatures and higher fO_2 values. The presence of other volatile species ($P_{CO_2} + P_{CO} < P$), dictates lower decomposition temperatures. The presence of water may stabilize iron hydroxide phases at lower temperatures. The redox couple required for this graphite formation mechanism can also potentially be provided by rhodochrosite (Mn-carbonate) where Mn^{2+} oxidizes to Mn^{4+}. However, rhodochrosite is stable at higher temperature than siderite, and probably did not play an important role in the formation of graphite in Isua metacarbonate rocks. A thorough discussion of the stability relations of rhodochrosite is given by Huebner (1969).

Garnet–staurolite–biotite assemblages and kyanite–biotite assemblages, as well as Fe–Mg partitioning between coexisting garnet and biotite, indicate a maximum temperature of ca. 550 °C and pressure of ca. 5 kbar for regional metamorphism in the ISB (Boak and Dymek, 1982). However, the metamorphic history of the ISB is complex, and several episodes of regional and contact metamorphism have been recognized (e.g.

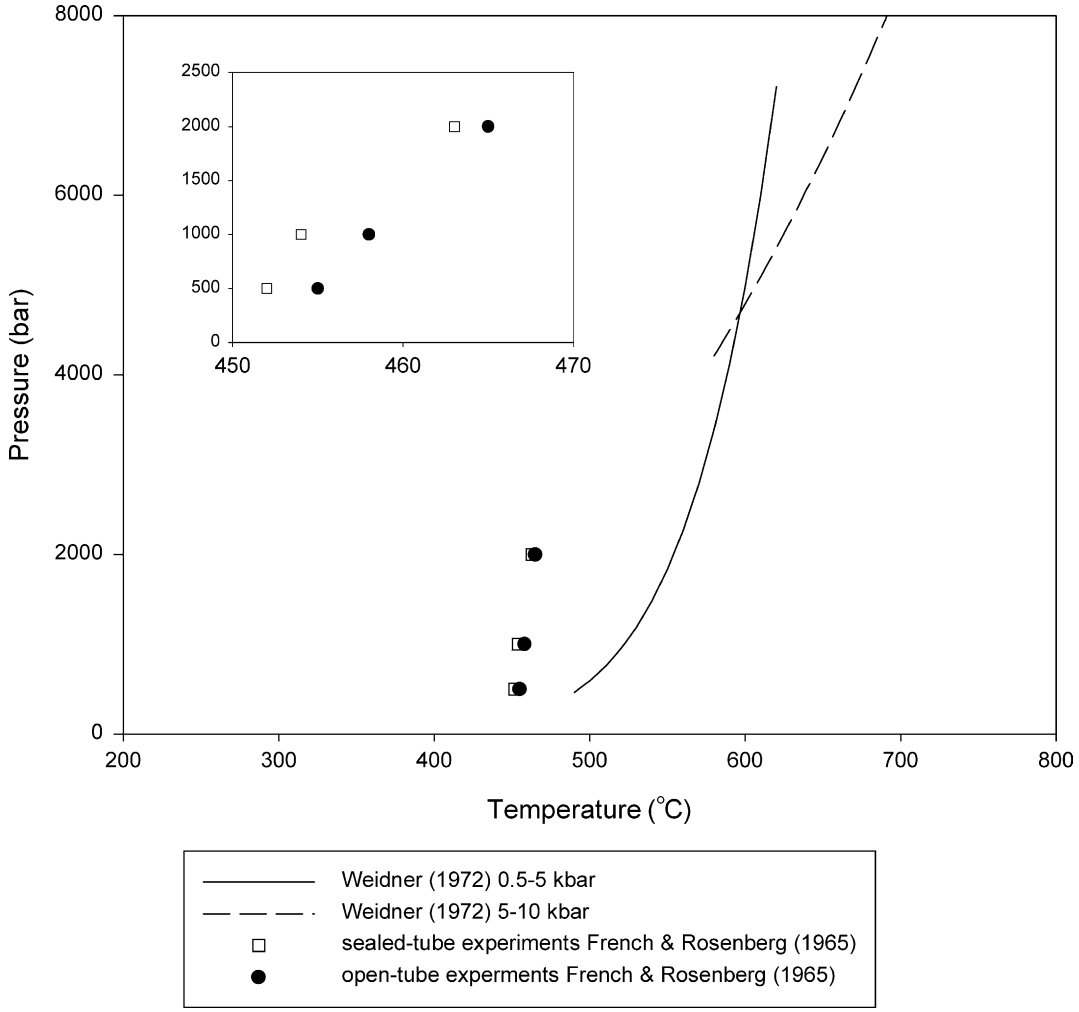

Fig. 7. Compilation from literature data of *P–T* conditions for the equilibrium siderite–magnetite–graphite–gas. Black dots show open-tube experiments (French and Rosenberg, 1965): $P = 500$ bar and $T = 455\,^{\circ}$C, $P = 1000$ bar and $T = 458\,^{\circ}$C, $P = 2000$ bar and $T = 465\,^{\circ}$C. Open squares show sealed-tube experiments (French and Rosenberg, 1965): $P = 500$ bar and $T = 452\,^{\circ}$C, $P = 1000$ bar and $T = 454\,^{\circ}$C, $P = 2000$ bar and 463 °C. The solid line represents the univariant curve $1/T(\mathrm{K}) = (1.739–0.1605 \log P)/1000$ for the interval $P = 500–5000$ bar, the dashed line represents the univariant curve $1/T(\mathrm{K}) = (2.934–0.486 \log P)/1000$ for the interval $P = 5000–10{,}000$ bar (Weidner, 1972).

Dymek and Klein, 1988). Recent garnet zonation studies have shown locally different metamorphic histories within the ISB (Rollinson, 2003). The occurrence of chlorite in many ISB rocks indicates widespread retrograde metamorphism at greenschist facies. Fe–Mg partitioning between garnet-rims and biotite indicate retrogression at a temperature of 460 °C. Although it is difficult to estimate with accuracy Fe–carbonate dissociation *P–T* conditions in the ISB, generally overlapping siderite dissociation requirements (Fig. 7) and the metamorphic history of the ISB suggest that the observed Fe-carbonate–magnetite–graphite association in metasomatic veins can be explained by thermal disproportionation of Fe-carbonate, and that the observed assemblages may represent an equilibrium under peak metamorphic conditions.

Perry and Ahmad (1977) first recognized graphite–magnetite–siderite associations in Isua carbonate-rich

rocks. Given the protolith interpretation of carbonates at the time, they argued that graphite in carbonate-rich BIFs in Isua could have been the product of the metamorphic alteration of an original siderite-rich sedimentary rock. The $\delta^{13}C$ of graphite in their samples ranged from −16 to −9.3‰, the carbonate $\delta^{13}C$ ranged from −4.1 to +1.8‰. The isotopic difference $\Delta_{carbonate-graphite}(\Delta = \delta^{13}C_{carbonate} - \delta^{13}C_{graphite})$ between their carbonate–graphite pairs was between 5.8 and 6.0‰, suggesting isotope equilibrium between the two phases at a peak metamorphic temperature of ca. 600 °C (according to the isotope equilibrium calculations of Bottinga, 1969). As carbon isotope exchange between carbonates and maturating organic matter would occur during prograde metamorphism until equilibrium is reached at peak metamorphic temperature, Perry and Ahmad (1977) concluded that it is impossible to use carbon isotopes to make a distinction between biologically derived graphite and abiogenic, siderite-derived graphite in these rocks. However, their conclusion was based on the assumption that carbonate-rich rocks were part of a sedimentary succession, and were closely related to cherts and BIFs. The current understanding that most carbonates occur in veins and are not sedimentary, but metasomatic in origin, and the data presented in this paper can now be used to draw firm conclusions about the origin of this graphite.

The ISB has experienced multiple regional and contact metamorphic events (Nutman et al., 1984, 1996) so it is reasonable to assume that siderite deposited in one metasomatic event can partially decompose during a later thermal event. Some of the veins studied here contain populations of carbonate minerals with different composition (Fig. 3), suggesting the involvement of multiple pulses of metasomatism with different fluid chemistries. Identification of Fe-bearing carbonates in close association with its reaction products, magnetite and graphite, in metacarbonate veins (Fig. 6) suggests either thermal disproportionation of carbonate near equilibrium *P* and *T*, or partial retrograde conversion of graphite and magnetite to carbonate. Highly graphitic samples MvZ6.4D1 and MvZ6.4D2 (Fig. 5a) from chlorite- and magnetite-dominated layers within a metacarbonate vein likely represent occasions where decomposition of Fe-bearing carbonate has proceeded to completion. It is possible that Dymek and Klein (1988) recognized such layers as their ‘graphitic iron formations’ with high MgO contents.

The reaction product of Fe-carbonate disproportionation under quartz-dominated conditions is grunerite (Fe-amphibole) rather than magnetite. When the original metacarbonate phase is a Fe-dolomite, a magnesium-rich amphibole, cummingtonite, will form instead of grunerite. This may explain the Fe-dolomite–cummingtonite–quartz–graphite association in the heavily carbonated chert sample AL17C. It was suggested earlier (Dymek and Klein, 1988) that graphite could form by a decarbonation reaction involving the formation of Fe-amphiboles.

6.2. Carbon isotope systematics:

When graphite forms from siderite under metamorphic conditions, carbon isotope equilibrium is expected between the two minerals. The equilibrium fractionation factor for siderite–graphite ($\alpha_{siderite-graphite} = {}^{13}C/{}^{12}C_{siderite}/{}^{13}C/{}^{12}C_{graphite}$) is assumed to be similar to the equilibrium fractionation factor ($\alpha_{calcite-graphite}$) for calcite–graphite. The calcite–graphite isotope equilibrium has been studied in great detail, because of its potential use as a geothermometer (Valley and O’Neil, 1981, 1984; Kitchen and Valley, 1995). Fig. 8 presents a compilation (modified from Kitchen and Valley, 1995) of different datasets showing $\alpha_{calcite-graphite}$ for different temperatures obtained by theoretical calculations (Ohmoto and Rye, 1979; Polyakov and Kharlashina, 1995), rock analyses (Valley and O’Neil, 1981; Dunn and Valley, 1992) and laboratory experiments (Chacko et al., 1991; Scheele and Hoefs, 1992). These plots (Fig. 8) indicate a range of $1000 \ln \alpha_{calcite-graphite}$ values from 5 to 8‰ for the temperature range between 450 and 550 °C ($1000 \ln \alpha_{calcite-graphite}$ is approximately equal to $\Delta_{calcite-graphite}$). These $\Delta_{carbonate-graphite}$ estimates (here we generalize the isotope equilibrium between calcite and graphite to ‘carbonate’ and graphite) for amphibolite-facies conditions are consistent with our measurements of Isua metacarbonate samples. Our data show a carbon isotopic difference between carbonate and graphite of ca. 6‰ (Fig. 9), with two exceptions: samples AL7-2 (both AL7-2M and AL7-2C) and MvZ6.3A2, which have a $\Delta_{carbonate-graphite}$ value in the range of 8–10‰. A possible explanation for these values is isotopic re-equilibration during a later low-*T*

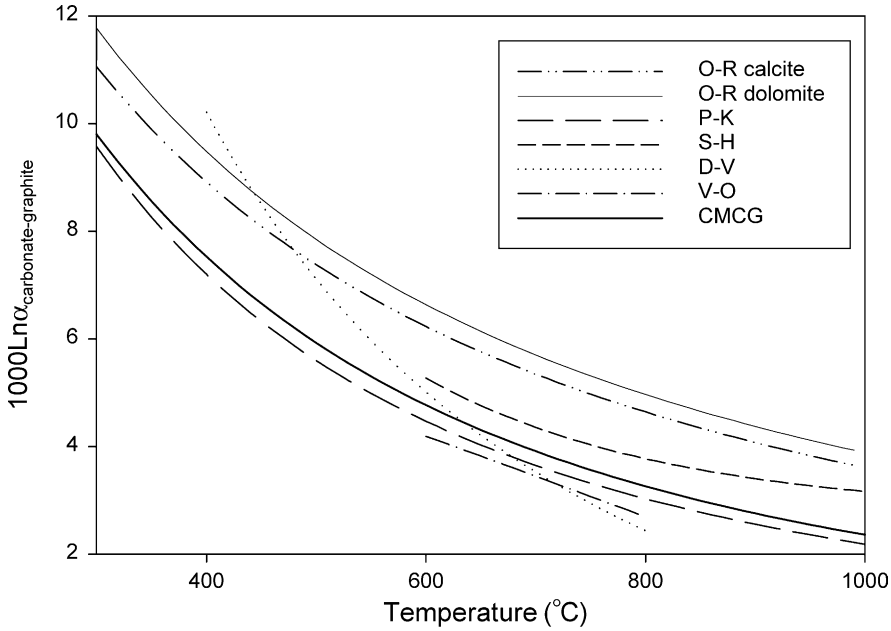

Fig. 8. Equilibrium carbon isotope fractionation between calcite and graphite as a function of temperature. Compilation of several studies (modified from Kitchen and Valley, 1995; O-R – Ohmoto and Rye, 1979) (also shown the equilibrium between graphite and dolomite); P-K – Polyakov and Kharlashina, 1995; S-H – Scheele and Hoefs, 1992; D-V – Dunn and Valley, 1992; V-O – Valley and O'Neil, 1981; CMCG – Chacko et al., 1991).

retrograde metamorphic event. Other effects may also have influenced the final carbon isotope ratio in graphite and associated carbonates; e.g. devolatilization and associated diffusional and/or kinetic effects.

Isotopic considerations thus support graphite formation by MgMn-siderite or Fe-dolomite disproportionation in Isua metacarbonates where the graphite acquired its $\delta^{13}C$ signature, between −12 and −10‰, by isotope fractionation near equilibrium.

The carbonate minerals themselves probably obtained their initial isotopic composition upon formation from CO_2 in the metamorphic fluid during metasomatism. It is difficult to estimate the $\delta^{13}C$ of this initial CO_2, since there are many factors that influenced the carbonate $\delta^{13}C$, including temperature regime of the metasomatic fluids, diffusive isotope fractionation during CO_2 transport, and cation composition of the specific metamorphic fluid.

Isotopically light graphitic globules have been described from graded beds (turbidities) in the western part of the ISB (Rosing, 1999; samples AL43-1, AL43-2, AL43-3 in this study). These rocks are characterized by significant graphite content (Fig. 5a), lack of Fe-bearing carbonate (Fig. 3a), and graphite $\delta^{13}C$ values that are significantly lower than our Fe-carbonate-derived graphite described above (Fig. 5b). A biogenic origin of this graphite can therefore not be excluded, although $\Delta_{carbonate-graphite}$ values in these samples are similar to the values found in some metacarbonate samples (Fig. 9). A recent study of W-isotopes (Schoenberg et al., 2002) suggested the possibility of a meteoritic component in these graded beds. It was hypothesized that the graphite there could ultimately have come from organic material in carbonaceous meteorites (average $\delta^{13}C$ of chondrites is −18‰). More evidence is needed to substantiate this suggestion which is in discord with the exceptionally low concentrations of platinum group elements (Koeberl et al., 2000) and with a different interpretation of the origin of a tungsten anomaly (Collerson et al., 2002).

6.3. Evaluation of graphite occurrences in the ISB

Biogenic material is enriched in ^{12}C relative to ^{13}C, due to a kinetic isotope effect that occurs during carbon

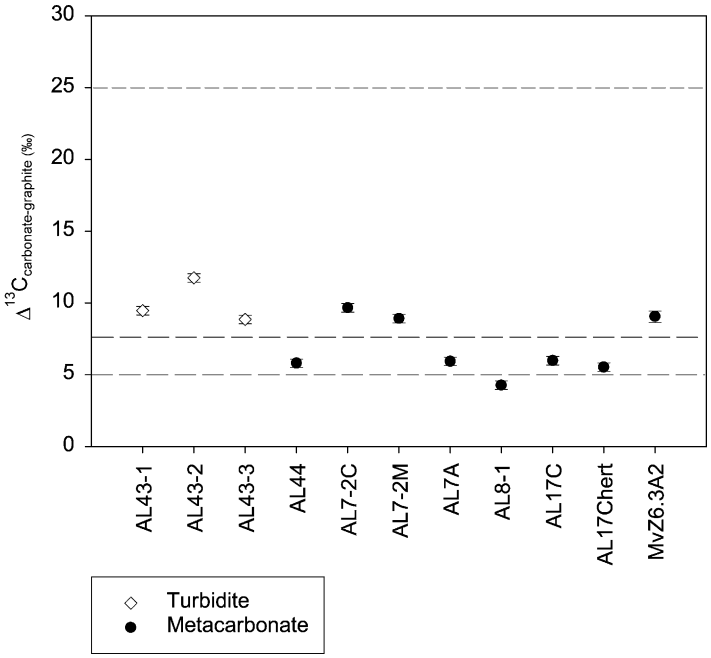

Fig. 9. Difference in $\delta^{13}C$ value between graphite and associated carbonate ($\Delta^{13}C_{carbonate-graphite}$) in metacarbonates, interpreted to reflect equilibrium isotope fractionation between these phases. The dashed lines indicate the range of values that would be expected when graphite forms from siderite disproportionation under the metamorphic conditions that Isua rocks have experienced (see Fig. 8). The dotted line shows the isotopic difference between kerogen ($\delta^{13}C = -25‰$) and carbonate ($\delta^{13}C = 0‰$) commonly observed in sediments over geologic time (Schidlowski, 2001). The $\Delta^{13}C$ value of sample AL17Chert was calculated using the $\delta^{13}C_{carbonate}$ value of the carbonate-rich part of sample AL17 (sample AL17C, see Table 1).

fixation in autotrophic organisms. The characteristic biogenic carbon isotope ratio is observed in recent organic sedimentary material on Earth, as well as in organic-rich sediments of different ages, even in rocks as old as 3.5 Ga (Schidlowski, 2001). Compilations of many $\delta^{13}C$ values in sedimentary rocks have led to the conclusion that, besides the fossil record, the geological carbon isotope record provides important evidence for the presence of a biosphere over geological time down to the Early Archean (Schidlowski et al., 1979; Hayes et al., 1983; Schidlowski, 1988, 2001).

The isotopic composition of graphite (average $\delta^{13}C = -15.3 \pm 6.2‰$) and associated carbonate (average $\delta^{13}C = -2.5 \pm 1.7‰$) in the ISB (Schidlowski et al., 1979) appeared consistent with the interpretation of metamorphically altered organic matter in marine carbonates. The offset of these original isotope values from typical marine carbonate (original $\delta^{13}C$ around. 0‰) and organic matter (assumed original $\delta^{13}C$ of ca. −25‰) was explained by isotope exchange during prograde metamorphism (Schidlowski et al., 1979), commonly seen in marbles (Hoefs and Frey, 1976; Valley and O'Neil, 1981, 1984; Scheele and Hoefs, 1992; Kitchen and Valley, 1995). The wide range of graphite $\delta^{13}C$ values seen in carbonate-rich Isua rocks was thought to be due to differential equilibration and it was concluded that some biogenic material could have escaped isotope exchange with carbonates or CO_2-bearing fluids during metamorphism.

This claim was seemingly supported by extremely low $\delta^{13}C$ values measured from graphite inclusions in apatite crystals ($\delta^{13}C = -30 \pm 3‰$ on average); graphite in apatite was interpreted to have escaped isotopic equilibration due to effective armoring (Mojzsis et al., 1996). However, these biogenic interpretations (Schidlowski et al., 1979; Mojzsis et al., 1996) were based on the assumption that the graphite-bearing Isua metacarbonate rocks, i.e. the rocks in which graphite was studied, formed part of a sedimentary sequence. The new view that most, if not all, carbonate in the

ISB is metasomatically emplaced (Rose et al., 1996), precludes carbonate-rich Isua rocks from providing information about 3.8 Ga biologic activity. The petrographic and isotopic evidence presented above points to epigenetic graphite formation through Fe-carbonate dissociation in Isua metacarbonates.

Graphite inclusions in apatite do not serve as biomarkers in Isua rocks, because they occur only in Fe-carbonate-containing metacarbonate rocks and are never found in metasedimentary BIFs or cherts (Lepland et al., 2002; van Zuilen et al., 2002). Mojzsis et al. (1996) studied graphite inclusions in apatite crystals from a rock (sample I-3381) which was at the time interpreted as a BIF. However, this rock has recently been reinterpreted as a metacarbonate (details are provided in Lepland et al., 2002; van Zuilen et al., 2002). In Isua metacarbonate samples studied here, as well as sample I-3381, Fe-carbonate-derived graphite is found as inclusions in all mineral phases including apatite (Fig. 6e). Although the mechanism for low $\delta^{13}C$ of graphite inclusions in apatite (Mojzsis et al., 1996) currently remains unexplained, it is clear from petrographic analysis alone that this graphite does not represent remnants of ancient life.

van Zuilen et al. (2002) found the Isua BIFs and cherts to have extremely low contents of reduced carbon. Stepped-heating-combustion experiments showed that the small amount of reduced carbon in these metasediments is isotopically light, but derives from recent organic contamination and not from ancient biogenic graphite. This casts doubt on the earlier findings of biogenic graphite obtained by the sealed-tube combustion experiments (Oehler and Smith, 1977; Perry and Ahmad, 1977; Schidlowski et al., 1979; Hayes et al., 1983).

A recent ion microprobe study by Ueno et al. (2002) reporting $\delta^{13}C$ values for graphite from Isua metasediments and carbonate rocks, show a large isotopic heterogeneity of graphite, from −18 to +2‰, on a millimeter-scale. These authors consider both biogenic and abiogenic graphite formation mechanisms and conclude that neither of these can be excluded. Mineralogic and petrographic data from their samples, however, may suggest metasomatic influences and highlight the need for careful consideration of graphite formation by decarbonation processes.

Graphite occurrences have also been reported in altered ultramafic rocks in the ISB. Naraoka et al. (1996) analyzed graphite with $\delta^{13}C = -12‰$ in a talc schist, and suggested serpentinization of an ultramafic body as a mechanism for the formation of this graphite.

7. Conclusions

The present study shows that graphite in rocks of the Isua Supracrustal Belt occurs abundantly in secondary metasomatic carbonate veins. Field evidence, micropetrographic analysis and carbon isotope signatures indicate that this graphite was formed by disproportionation of Fe-bearing carbonates under amphibolite-facies conditions, hence it can not be used as evidence for ancient life. As a result our study calls for the reassessment of earlier interpretations of traces of life from 3.8 Ga (Schidlowski et al., 1979; Mojzsis et al., 1996) derived from studies of these graphitic metacarbonates.

We suggest that the isotopic composition of graphite in supracrustal rocks subjected to high-grade metamorphism does not in general, serve as a reliable biomarker, since epigenetic processes may yield graphite with isotopic characteristics that overlap with isotopic signatures of metamorphosed organism remains.

In conclusion, we emphasize that our study does not categorically negate the possibility that biogenic graphite could be retained in the 3.8 Ga ISB. Our study merely illustrates how interpretations based on the isotopic composition of graphite are best understood when placed in proper geologic context. As pointed out by Craig (1953), geological evidence may help to evaluate the isotopic variation in graphite, but the reverse is not necessarily true.

Acknowledgements

We thank Bruce Deck for assistance in the carbon isotope analysis of graphite, and P. W. U. Appel for providing coordination, facilities and support for field work as part of the Isua Multidisciplinary Research Project. Furthermore we express our thanks to the Danish Natural Science Research Council, to the Commission for Scientific Research in Greenland and to the Bureau of Minerals and Petroleum, Nuuk, Greenland, for generous support of the Isua

Multidisciplinary Research Project, from which this is a contribution. NASA Exobiology grants NAGW-1035 and NAG5-4563, and an extended grant from the Marianne and Marcus Wallenberg Foundation (for A.L) are gratefully acknowledged. Constructive comments on the manuscript were kindly provided by J.F. Kasting, S. Moorbath, P.W.U. Appel, J. Touret, and an anonymous reviewer.

References

Appel, P.W.U., 1980. On the early Archaean Isua iron formation, West Greenland. Precambrian Res. 11, 73–87.

Appel, P.W.U., Fedo, C.M., Moorbath, S., Myers, J.S., 1998. Recognizable primary volcanic and sedimentary features in a low-strain domain of the highly deformed, oldest known (~3.7–3.8 Gyr) Greenstone Belt, Isua, West Greenland. Terra Nova 10, 57–62.

Boak, J.L., Dymek, R.F., 1982. Metamorphism of the ca. 3800 Ma supracrustal rocks at Isua, West Greenland: implications for early Archaean crustal evolution. Earth Planet. Sci. Lett. 59, 155–176.

Bottinga, Y., 1969. Calculated fractionation factors for carbon and hydrogen isotope exchange in the system calcite–carbon dioxide–graphite–methane–hydrogen–water vapor. Geochim. Cosmochim. Acta 33, 49–64.

Chacko, T., Mayeda, T.K., Clayton, R.N., Goldsmith, J.R., 1991. Oxygen and carbon isotope fractionations between CO_2 and calcite. Geochim. Cosmochim. Acta 55, 2867–2882.

Collerson, K.D., Schoenberg, R., Kamber, B.S., 2002. Unradiogenic W in kimberlites. Direct evidence for core–mantle interaction. Geochim. Cosmochim. Acta 66, A148.

Craig, H., 1953. The geochemistry of the stable carbon isotopes. Geochim. Cosmochim. Acta 3, 53–92.

Craig, H., 1957. Isotopic standards for carbon and oxygen and correction factors for mass-spectrometric analysis of carbon dioxide. Geochim. Cosmochim. Acta 12, 133–149.

Dimroth, E., 1982. The oldest rocks on Earth: stratigraphy and sedimentology of the 3.8 billion years old Isua supracrustal sequence. In: Sidorenko, A.V. (Ed.), Sedimentary Geology of the Highly Metamorphosed Precambrian Complexes. Nauka, Moscow, pp. 16–27.

Dunn, S.R., Valley, J.W., 1992. Calcite–graphite isotope thermometry: a test for polymetamorphism in marble, Tudor gabbro aureole, Ontario, Canada. J. Metamorph. Geol. 10, 487–501.

Dymek, R.F., Klein, C., 1988. Chemistry, petrology and origin of banded iron formation lithologies from the 3800 Ma Isua Supracrustal Belt, West Greenland. Precambrian Res. 39, 247–302.

Fedo, C.M., 2000. Setting and origin for problematic rocks from the >3.7 Ga Isua Greenstone Belt, southern West Greenland: Earth's oldest coarse clastic sediments. Precambrian Res. 101, 69–78.

Fedo, C.M., Myers, J.S., Appel, P.W.U., 2001. Depositional setting and paleogeographic implications of Earth's oldest supracrustal rocks the >3.7 Ga Isua Greenstone belt, West Greenland. Sediment. Geol. 141, 61–77.

French, B.M., 1971. Stability relations of siderite ($FeCO_3$) in the system Fe–C–O. Am. J. Sci. 271, 37–78.

French, B.M., Eugster, H.P., 1965. Experimental control of oxygen fugacities by graphite–gas equilibriums. J. Geophys. Res. 70, 1529–1539.

French, B.M., Rosenberg, P.E., 1965. Siderite ($FeCO_3$): thermal decomposition in equilibrium with graphite. Science 147, 1283–1284.

Hayes, J.M., Kaplan, I.R., Wedeking, W., 1983. Precambrian organic geochemistry, preservation of the record. In: Schopf, J.W. (Ed.), Earth's earliest Biosphere, its Origin and Evolution. Princeton University Press, Princeton, NJ, pp. 93–134.

Hoefs, J., Frey, M., 1976. The isotopic composition of carbonaceous matter in a metamorphic profile from the Swiss Alps. Geochim. Cosmochim. Acta 40, 945–951.

Huebner, J.S., 1969. Stability relations of rhodochrosite in the system manganese–carbon–oxygen. Am. Mineral. 54, 457–481.

James, H.L., 1954. Sedimentary facies of iron formation. Econ. Geol. 49, 235–293.

Kitchen, N.E., Valley, J.W., 1995. Carbon isotope thermometry in marbles of the Adirondack Mountains, New York. J. Metamorph. Geol. 13, 577–594.

Koeberl, C., Reimold, W.U., McDonald, I., Rosing, M., 2000. Search for petrographic and geochemical evidence for the late heavy bombardment on Earth in Early Archean rocks from Isua, Greenland. In: Gilmor, I., Koeberl, C. (Eds.), Impact and the Early Earth. Lecture Notes in Earth Sciences, vol. 91. Springer, Heidelberg, Berlin, pp. 73–97.

Komiya, T., Maruyama, S., Masuda, T., Nohda, S., Hayashi, M., Okamoto, K., 1999. Plate tectonics at 3.8–3.7 Ga: field evidence from the Isua accretionary complex southern West Greenland. J. Geol. 107, 515–554.

Lepland, A., Arrhenius, G., Cornell, D., 2002. Apatite in Early Archean Isua supracrustal rocks, southern West Greenland: its origin, association with graphite and potential as a biomarker. Precambrian Res. 118, 221–241.

McCrea, J.M., 1950. On the isotopic chemistry of carbonates and a paleotemperature scale. J. Chem. Phys. 18, 849–857.

Mel'nik, Y.P., 1982. Precambrian banded iron-formations, physicochemical conditions of formation. Developments in Precambrian Geology, vol. 5. Elsevier, Amsterdam.

Mojzsis, S.J., Arrhenius, G., McKeegan, K.D., Harrison, T.M., Nutman, A.P., Friend, C.R.L., 1996. Evidence for life on Earth before 3800 million years ago. Nature 384, 55–59.

Moorbath, S., O'Nions, R.K., Pankhurst, R.J., 1973. Early Archaean age for the Isua iron formation, West Greenland. Nature 245, 138–139.

Muan, A., 1958. Phase equilibria at high temperatures in oxide systems involving changes in oxidation states. Am. J. Sci. 256, 171–207.

Myers, J.S., 2001. Protoliths of the 3.8–3.7 Ga Isua greenstone belt, West Greenland. Precambrian Res. 105, 129–141.

Myers, J.S., Crowley, J.L., 2000. Vestiges of life in the oldest Greenland rocks? A review of early Archaean geology in

the Godthaabsfjord region, and reappraisal of field evidence for >3850 Ma life on Akilia. Precambrian Res. 103, 101–124.

Nagy, B., Zumberge, J.E., Nagy, L.A., 1975. Abiotic, graphitic microstructures in micaceous metaquartzite about 3760 million years old from Southwestern Greenland: implications for Early Precambrian micorfossils. Proceedings of the U.S. National Academy of Sciences 72, 1206–1209.

Naraoka, H., Ohtake, M., Maruyama, S., Ohmoto, H., 1996. Non-biogenic graphite in 3.8-Ga metamorphic rocks from the Isua district, Greenland. Chem. Geol. 133, 251–260.

Nutman, A.P., 1986. The early Archaean to Proterozoic history of the Isuakasia area, southern West Greenland. Grønlands Geologiske Undersøgelse Bull. 154.

Nutman, A.P., Allaart, J.H., Bridgwater, D., Dimroth, E., Rosing, M., 1984. Stratigraphic and geochemical evidence for the depositional environment of the early Archaean Isua Supracrustal Belt southern West Greenland. Precambrian Res. 25, 365–396.

Nutman, A.P., McGregor, V.R., Friend, C.R.L., Bennett, V.C., Kinny, P.D., 1996. The Itsaq Gneiss Complex of southern West Greenland; the world's most extensive record of early crustal evolution (3900–3600 Ma). Precambrian Res. 78, 1–39.

Oehler, D.Z., Smith, J.W., 1977. Isotopic composition of reduced and oxidized carbon in Early Archaean rocks from Isua, Greenland. Precambrian Res. 5, 221–228.

Ohmoto, H., Rye, R.O., 1979. Isotopes of sulfur and carbon. In: Barnes, H.L. (Ed.), Geochemistry of Hydrothermal Ore Deposits. Wiley, New York, pp. 509–567.

Perry Jr., E.C., Ahmad, S.N., 1977. Carbon isotope composition of graphite and carbonate minerals from 3.8 AE metamorphosed sediments, Isuakasia, Greenland. Earth Planet. Sci. Lett. 36, 280–284.

Polyakov, V.B., Kharlashina, N.N., 1995. The use of heat capacity data to calculate carbon isotope fractionation between graphite, diamond, and carbon dioxide: a new approach. Geochim. Cosmochim. Acta 59, 2561–2572.

Rollinson, H., 2003. Garnet growth chronologies indicate a complex metamorphic history for the Isua Greenstone Belt, West Greenland. Precambrian Res. 126, 181–196.

Rose, N.M., Rosing, M.T., Bridgwater, D., 1996. The origin of metacarbonate rocks in the Archaean Isua Supracrustal Belt, West Greenland. Am. J. Sci. 296, 1004–1044.

Rosenbaum, J., Sheppard, S.M.F., 1986. An isotopic study of siderites, dolomites and ankerites at high temperatures. Geochim. Cosmochim. Acta 50, 1147–1150.

Rosing, M.T., 1999. ^{13}C-depleted carbon microparticles in >3700-Ma sea-floor sedimentary rocks from West Greenland. Science 283, 674–676.

Rosing, M.T., Rose, N.M., 1993. The role of ultramafic rocks in regulating the concentrations of volatile and non-volatile components during deep crustal metamorphism. Chem. Geol. 108, 187–200.

Rosing, M.T., Rose, N.M., Bridgwater, D., Thomsen, H.S., 1996. Earliest part of Earth's stratigraphic record: a reappraisal of the >3.7 Ga Isua (Greenland) supracrustal sequence. Geology 24 (1), 43–46.

Scheele, N., Hoefs, J., 1992. Carbon isotope fractionation between calcite, graphite and CO_2: an experimental study. Contrib. Mineral Petrol. 112, 35–45.

Schidlowski, M., 1988. A 3800-million-year isotopic record of life from carbon in sedimentary rocks. Nature 333, 1988.

Schidlowski, M., 2001. Carbon isotopes as biogeochemical recorders of life over 3.8 Ga of Earth history: evolution of a concept. Precambrian Res. 106, 117–134.

Schidlowski, M., Appel, P.W.U., Eichmann, R., Junge, C.E., 1979. Carbon isotope geochemistry of the 3.7×10^{-9} yr-old Isua sediments, West Greenland: implications for the Archaean carbon and oxygen cycles. Geochim. Cosmochim. Acta 43, 189–199.

Schoenberg, R., Kamber, B.S., Collerson, K.D., Moorbath, S., 2002. Tungsten isotope evidence from ~3.8-Gyr metamorphosed sediments for early meteorite bombardment of the Earth. Nature 418, 403–405.

Ueno, Y., Yurimoto, H., Yoshioka, H., Komiya, T., Maruyama, S., 2002. Ion microprobe analysis of graphite from ca. 3.8 Ga metasediments, Isua Supracrustal Belt, West Greenland: relationship between metamorphism and carbon isotopic composition. Geochim. Cosmochim. Acta 66, 1257–1268.

Valley, J.W., O'Neil, J.R., 1981. ^{13}C/^{12}C exchange between calcite and graphite: a possible thermometer in Grenville marbles. Geochim. Cosmochim. Acta 45, 411–419.

Valley, J.W., O'Neil, J.R., 1984. Fluid heterogeneity during granulite facies metamorphism in the Adirondacks: stable isotope evidence. Contrib. Mineral. Petrol. 85, 158–173.

van Zuilen, M.A., Lepland, A., Arrhenius, G., 2002. Reassessing the evidence for the earliest traces of life. Nature 418, 627–630.

Wedeking, W., Hayes, J.M., Matzigkeit, U., 1983. Procedures of organic geochemical analysis. In: Schopf, J.W. (Ed.), Earth's Earliest Biosphere. Princeton University Press, Princeton, NJ, pp. 428–443.

Weidner, J.R., 1972. Equilibria in the system Fe–C–O part I: siderite–magnetite–carbon–vapor equilibrium from 500 to 10,000 bars. Am. J. Sci. 272, 735–751.

Yui, S., 1966. Decomposition of siderite to magnetite at lower oxygen fugacities: a thermodynamical interpretation and geological implications. Econ. Geol. 61, 768–776.